

Hard exudates referral system in eye fundus utilizing speeded up robust features

Syed Ali Gohar Naqvi, Hafiz Muhammad Faisal Zafar, Ihsanul Haq

International Islamic University (IIUI), H-10, Islamabad, Pakistan

Correspondence to: Syed Ali Gohar Naqvi. International Islamic University (IIUI), H-10, Islamabad, Pakistan. syed.phdee37@iiu.edu.pk

Received: 2016-06-30 Accepted: 2016-12-07

Abstract

• In the paper a referral system to assist the medical experts in the screening/referral of diabetic retinopathy is suggested. The system has been developed by a sequential use of different existing mathematical techniques. These techniques involve speeded up robust features (SURF), K-means clustering and visual dictionaries (VD). Three databases are mixed to test the working of the system when the sources are dissimilar. When experiments were performed an area under the curve (AUC) of 0.9343 was attained. The results acquired from the system are promising.

• **KEYWORDS:** referral system; speeded up robust features; eye; fundus; visual dictionaries

DOI:10.18240/ijo.2017.07.24

Naqvi SA, Zafar HMF, Haq I. Hard exudates referral system in eye fundus utilizing speeded up robust features. *Int J Ophthalmol* 2017; 10(7):1171-1174

INTRODUCTION

Hard exudate is the fundamental artifact which exists in diabetic patients most of the times. In many cases, the manifestation of these artifacts confirms that the patient should seek medical help from a medical expert. Manifestation of hard exudates may prove helpful in screening of diabetic retinopathy. The patients left untreated may encounter blurred vision or blindness. To assist the overloaded medical experts in screening, a referral system for hard exudates is required.

The presented system uses speeded up robust features (SURF)^[1] to acquire basic features from images, K-means clustering^[2] for developing visual dictionaries (VD)^[3] and for classification support vector machine (SVM)^[4] is employed.

Sopharak *et al*^[5] developed a system only utilizing basic image processing techniques such as filtering and contrast enhancement. For their system to perform optimally the pixels

of both classes *i.e.* artifact and normal must have significant difference in their intensities. García *et al*^[6] proposed a system based on features like average and standard deviation of artifact and normal classes. They also utilized various classifiers and machine learning techniques. Sopharak *et al*^[7] and Dupas *et al*^[8] used fuzzy clustering along with carefully chosen features like standard deviation of intensities and hue *etc* for detection purposes. Dynamic thresholding and different statistical techniques were used by Sánchez *et al*^[9] for the same problem. Another system proposed by Welfer *et al*^[10] used morphological operations and watershed transform in LUV colorspace for the same purpose. In LUV color space, L is the luminance component and U and V components provide color information. Sanchez *et al*^[11] proposed another system which required patient's contextual information and SVM as a classifier. Chen *et al*^[12] proposed an algorithm in which different histogram and morphological operations were suggested. Garcia *et al*^[13] employed logistic regression along with radial basis function classifier for addressing the problem. Kayal and Banerjee^[14] also suggested basic image processing techniques in his method. Naqvi *et al*^[15] used scale-invariant feature transform (SIFT) feature and SVM for extraction of hard exudates. In the method no preprocessing is required.

METHODS

Suggested Technique The training and testing phases of the suggested system is given in the following sections.

Training phase The first step involved in the training phase is the extraction of point of interests (POIs). For this purpose SURF is employed. SURF can extract relatively huge number of POIs from an image. In image processing systems the features in the vicinity of POIs are more advantageous than the global features of the image^[16]. In Figure 1A and 1B, a fundus image along with few POIs detected on the same image is displayed. Before the training phase three medical experts annotated the images to point out the artifact and normal regions. They also annotated the optic disc region in the training images. Utilizing SURF, a number of descriptors can be found from a fundus image. These descriptors act as low level features (LLF) as they are in raw form and cannot be fed into the classifier. Let an arbitrary training image I_i where $i \in \{1, 2, 3, \dots, m\}$ and m is the total number of training images. d_a and d_n are the descriptors or LLF of I_i found through SURF. It should be noted that d_a are the LLF

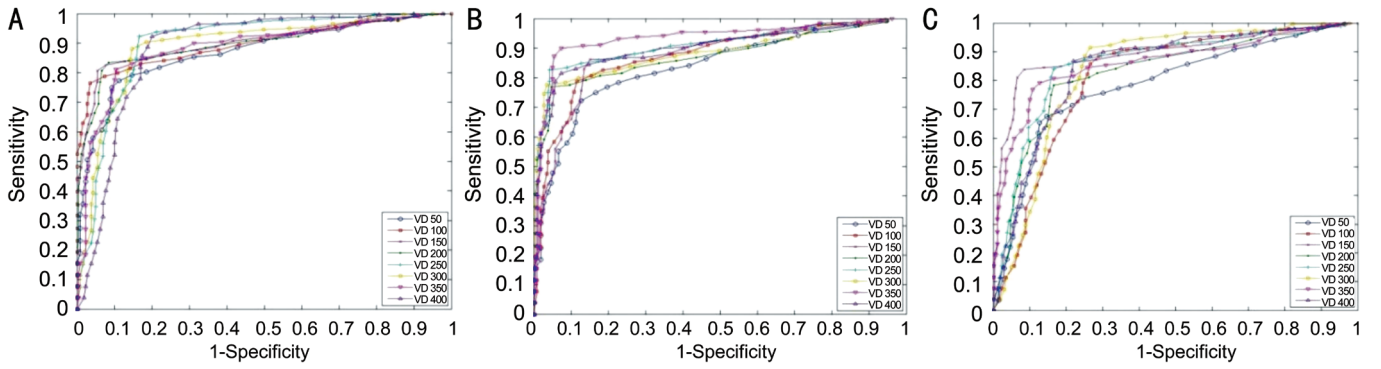


Figure 1 ROC for different VDs in mixture of image databases using SVM within (A) RS1 (B) RS2 (C) RS3.

Table 1 Databases utilized in the work

Database	Useful images (containing hard exudates)	Resolution (pixels)	Developer
DR1	234	640×480	Federal University of Sao Paulo (UNIFESP)
DR2	79	867×575	Federal University of Sao Paulo (UNIFESP)
Diaretdbl	46	1500×1152	Kuopio University Hospital

of regions of image I_i containing artifact while d_n represents the LLF from regions of image I_i considered normal by the experts. Here $a \in \{1, 2, 3, \dots, q\}$ and $n \in \{1, 2, 3, \dots, p\}$, q and p are total LLF gathered from training images and d_a , $d_n \in \mathcal{Y}$ exists in y -dimensional space. Utilizing the LLF, d_a and d_n visual dictionary $V = \{v_1, v_2, v_3, \dots, v_k\}$ is constructed through K-means clustering. v_k refers to a signal visual codeword from V . Following steps involve the quantization and spooling of I_i based on V . For this, first each d_a , $d_n \in \mathcal{Y}$ is mapped onto the V . This transforms the low level d_a and d_n onto a representation bases upon visual codewords of V . Mathematically this can be represented as $f: \mathcal{Y} \rightarrow \mathcal{K}$, $f(d_a) = \mu_a$ and $f(d_n) = \mu_n$. μ 's are acquired through the 'hard assignment'^[17] of LLF to the nearest codeword of V i.e.:

$$\mu_{qk} = 1 \text{ if } q = \arg \min_k \|v_k - d\|^2 \text{ else } q = 0$$

Here $\mu_{q,k}$ is the q^{th} component of mid-level feature (MLF) that is now obtained and $d = \{d_a, d_n\}$, $\mu = \{\mu_a, \mu_n\}$, $l = n+p$. For feeding these features into SVM the spooling step is still required. These obtained features are considered as MLF.

In sum spooling the high level feature vector τ is found i.e.:

$$g(\{\mu_k\}) = \tau : \forall q, \tau_q = \sum_{k=1}^N \mu_{q,k} \text{ where } \tau \in \mathcal{K}$$

The features gathered at this point, in the form of τ 's are useful for the classifier and the classifier reports its decisions based on these high level features (HLF). The results are checked on a linear SVM^[4].

Testing phase In this phase the steps mentioned in training phase are again repeated but with the test images. However no new VDs are developed and the VDs of training phase are employed for the testing procedure.

Databases and Experiments

Choice of database To test the suggested system three databases have been employed i.e. Diaretdbl^[18], DR1^[19], DR2^[19]. The salient features of the databases are tabulated in Table 1.

Experiments In the experiments the images of the three databases i.e. DR1, DR2 and Diaretdbl are mixed. This is done to test the system in a more challenging situation where the sources of the images are dissimilar and the images are taken in different conditions. In the experiments 100 artifact images and 100 normal images are used for training purpose while the remaining is utilized in testing phase. Overall 359 (234+79+46) artifact and 359 randomly selected normal images are involved in the experiments. Mixing of images may induce a biasing effect on the system; therefore the method of random subsampling^[20] is utilized for testing the system. Three random sets named as RS1, RS2 and RS3 are used in the random subsampling. The system was also evaluated at different sizes of VDs i.e. VD50, VD100, VD150 to VD400.

RESULTS AND DISCUSSION

The results of the suggested system are shown in terms of sensitivity, specificity and accuracy^[21]. These results are obtained on three different RS and different sizes of the VDs. The area under the curve (AUC) of radio operating curve (ROC) has also been obtained. In the tests the average AUC within the VD has also been computed. Apart from this the standard deviation within the VD has also been calculated.

The top accuracy of 91.89% is recorded for VD350 and RS2. The maximum average AUC of 0.8942 (89.42%) is attained on VD350. The highest AUC of 0.9343(93.43%) is recorded for RS2 when VD350 is used. Figure 1 shows a view of the results of the experiments. The maximum sensitivity, specificity and accuracy of suggested system has been shown in Table 2.

From overall results gathered from the system, it is clear that the suggested system displays almost stable AUC on all RS for experiments. However, sometimes minutely poor performance can be observed on RS3 as compared to RS1 and RS2. The random mixing of the images gathered from different

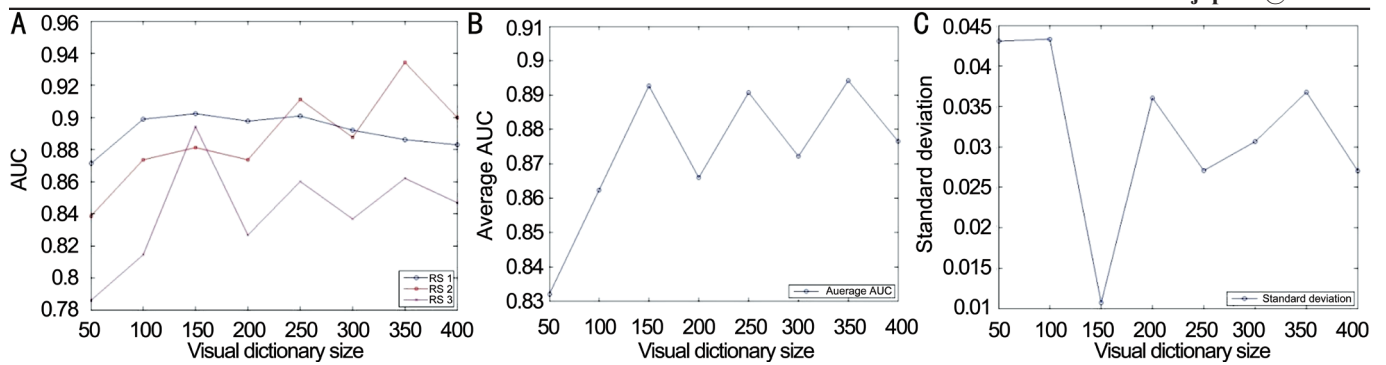


Figure 2 Statistics obtained from experiments A: AUC for RS1, RS2 and RS3 in mixture of image databases using SVM; B: Average AUC for RS1, RS2 and RS3 in mixture of image databases using SVM; C: Standard deviation for different VD sizes in mixture of image databases using SVM.

Table 2 Comparison with other methods %

Authors	Sensitivity	Specificity	Accuracy
Ricci <i>et al</i> ^[22]	-	-	96.46
Al-Diri <i>et al</i> ^[23]	72.82	95.51	-
Marin <i>et al</i> ^[24]	-	-	72.82
Lam <i>et al</i> ^[25]	-	-	94.74
Naqvi <i>et al</i> ^[15]	92.70	81.02	87.23
Presented work	93.82 (max)	96.53 (max)	91.83 (max)

datasets is the cause for the observation. For both categories of experiments the value of average AUC also remains almost stable when the size of VD increases from VD50 to VD400. In experiments minor fluctuations are observed in the values of standard deviation with in the VDs. This is again due to the selection of different RS by the computer. The mentioned facts and statistics obtained from experiments are further elucidate in detail through graphical view of Figure 2.

In the paper, it has been elaborated that the patients of diabetes are increasing day by day. To remove the enormous load from the medical experts a referral system is suggested and is developed by making use of various mathematical techniques. To better evaluate the system, when the images belong to various sources, it has also been checked by combining various databases. The working of the system is evaluated with different RS and various sizes of VDs. The suggested system shows promising results. A maximum AUC of 0.9343 (93.43%) is noted with VD350.

ACKNOWLEDGEMENTS

Conflicts of Interest: Naqvi SA, None; Zafar HMF, None; Haq I, None.

REFERENCES

- 1 Bay H, Tuytelaars T, Gool LV. *SURF: speeded up robust features*. European Conference on Computer Vision 2006:404-417.
- 2 Lloyd S. Least squares quantization in PCM. *IEEE Trans Inf Theory* 1982;28(2):129-137.
- 3 Winn J, Criminisi A, Minka T. *Object categorization by learned universal visual dictionary*. Proceedings of the Tenth IEEE International Conference on Computer Vision 2005;2:1800-1807.

- 4 Bishop C. *Pattern recognition and machine learning*. 1st ed. Springer, 2006.
- 5 Sopharak A, Uyyanonvara B, Barman S, Williamson T. Automatic detection of diabetic retinopathy exudates from non-dilated retinal images using mathematical morphology methods. *Comput Med Imaging Graph* 2008;32(8):720-727.
- 6 García M, Sánchez CI, López MI, Abásolo D, Hornero R. Neural network based detection of hard exudates in retinal images. *Comput Methods Programs Biomed* 2009;93(1):9-19.
- 7 Sopharak A, Uyyanonvara B, Barman S. Automatic exudate detection from non-dilated diabetic retinopathy retinal images using fuzzy C-means clustering. *Sensors (Basel)* 2009;9(3):2148-2161.
- 8 Dupas B, Walter T, Erginay A, Ordonez R, Deb-Joardar N, Gain P, Klein JC, Massin P. Evaluation of automated fundus photograph analysis algorithms for detecting microaneurysms, haemorrhages and exudates, and of a computer-assisted diagnostic system for grading diabetic retinopathy. *Diabetes Metab* 2010;36(3):213-220.
- 9 Sánchez CI, García M, Mayo A, López MI, Hornero R. Retinal image analysis based on mixture models to detect hard exudates. *Med Image Anal* 2009;13(4):650-658.
- 10 Welfer D, Scharcanski J, Marinho DR. A coarse-to-fine strategy for automatically detecting exudates in color eye fundus images. *Comput Med Imaging Graph* 2010;34(3):228-235.
- 11 Sanchez CI, Niemeijer M, Suttorp Schulten MSA, Abramoff M, van Ginneken BV. *Improving hard exudate detection in retinal images through a combination of local and contextual information*. Proceedings of the 2010 IEEE International Conference on Biomedical Imaging 2010:5-8.
- 12 Chen X, Wei B, Wu XQ, Dai BS. *A novel method for automatic hard exudates detection in color retinal images*. International Conference on Machine Learning and Cybernetics 2012:1175-1181.
- 13 Garcia M, Valverde C, Lopez MI, Poza J, Hornero R. Comparison of logistic regression and neural network classifiers in the detection of hard exudates in retinal images. *Conf Proc IEEE Eng Med Biol Soc* 2013; 2013:5891-5894.
- 14 Kayal D, Banerjee S. *A new dynamic thresholding based technique for detection of hard exudates in digital retinal fundus image*. International Conference on Signal Processing and Integrated Networks 2014:141-144.
- 15 Naqvi SA, Zafar MF, Haq Iu. Referral system for hard exudates in eye fundus. *Comput Biol Med* 2015;64:217-235.

- 16 Lowe D. Distinctive image features from scale-invariant keypoints. *Int J Comput Vis* 2004;60(2):91-110.
- 17 Kearns M, Mansour Y, Andrew Y. *An information-theoretic analysis of hard and soft assignment methods for clustering*. Proceedings of the Thirteen Conference on Uncertainty in Artificial Intelligence 1997:282-293.
- 18 Diaretdb1 Dataset. Available at <http://www2.it.lut.fi/project/imageret/diaretdb1/>; Accessed on 13 February 2016.
- 19 DR1, DR2 Datasets. Available at <http://www.recod.ic.unicamp.br/site/asdror>; Accessed on 13 February 2016.
- 20 Picard R, Cook RD. Cross-validation regression models. *J Am Stat Assoc* 1984;79.
- 21 Vidakovic B. *Sensitivity, specificity, and relatives*. Statistics for Bioengineering Sciences, Springer Texts in Statistics 2011:109-130.
- 22 Ricci E, Perfetti R. Retinal blood vessel segmentation using line operators and support vector classification. *IEEE Trans Med Imaging* 2007;26(10):1357-1365.
- 23 Al-Diri B, Hunter A, Steel D. An active contour model for segmenting and measuring retinal vessels. *IEEE Trans Med Imaging* 2009;28(9):1488-1497.
- 24 Marin D, Aquino A, Gegundez M, Bravo J. A new supervised method for blood vessel segmentation in retinal images by using gray-level and moment invariants-based features. *IEEE Trans Med Imaging* 2011;30(1):146-158.
- 25 Lam BS, Gao Y, Liew AW. General retinal vessel segmentation using regularization-based multiconcavity modeling. *IEEE Trans Med Imaging* 2010;29(7):1369-1381.